IEEE Access
Multidisciplinary ⋮ Rapid Review ⋮ Open Access Journal

Received 1 February 2024, accepted 11 February 2024, date of publication 23 February 2024, date of current version 26 March 2024.

Digital Object Identifier 10.1109/ACCESS.2024.3369247

RESEARCH ARTICLE

Data Transmission Analysis and Communication Scheme Design for TianQin Mission

ZHAOXIANG YI, LIN SUN, (Graduate Student Member, IEEE), AND MENG JIANG, (Graduate Student Member, IEEE)

MOE Key Laboratory of TianQin Mission, TianQin Research Center for Gravitational Physics, School of Physics and Astronomy, Frontiers Science Center for TianQin, Gravitational Wave Research Center of CNSA, Sun Yat-sen University (Zhuhai Campus), Zhuhai 519082, China

Corresponding author: Lin Sun (sunlin35@mail2.sysu.edu.cn)

This work was supported by the National Key Research and Development Program of China under Grant 2022YFC2204602.

ABSTRACT Compared with ground-based gravitational wave detection, space-based gravitational wave detection has become a research hotspot because of its abundant wave sources. However, how to reliably transmit the detection data, obtained by the space gravitational wave detector, back to the ground station from a distance of 10^5 kilometers is a huge challenge. In this paper, the visibility analysis and link budget are carried out for the data transmission of gravitational wave detection in geocentric orbit space, and a high real-time data transmission scheme is provided to support the mHz band gravitational wave detection. In more detail, we firstly establish a theoretical model for visibility analysis and link budget based on spacecraft dynamics model and communication link model. Secondly, through visibility simulation and calculation, we obtained the average communication time per day, and found that the Zhuhai station has a more uniform distribution of communication time compared with other ground stations. Subsequently, the link budget model indicates that link performance is largely determined by various gains and attenuations during the link process, which are related to the link working frequency band and resource allocation. Comparing the differences on gain and attenuation between X-band and Ka-band, we design an X-band communication scheme with the transmission rate of 1Mbps and bit error rate of 10^{-5}. The calculation results also show that the communication scheme has a C/N_0 margin of 4.10 dB, which meets the data transmission requirements of TianQin. Finally, the research shows that compared with the heliocentric orbit of LISA, the geocentric orbit of TianQin has obvious advantages in transmission delay, communication time and real-time performance of data transmission, avoiding the antenna pointing issues and is more conducive to the multi-messenger detection of large astronomical events.

INDEX TERMS Gravitational waves, link budget, satellite communication, visibility analysis.

I. INTRODUCTION

Albert Einstein proposed the general relativity in 1916. One of the ideas is that the asymmetric motion of mass will cause ripples in the gravitational field, whose space-time distortions propagate at the speed of light, called gravitational wave (GW). In 2016, Laser Interferometer Gravitational-Wave Observatory (LIGO) announced that it had successfully detected GW from two stations on the ground for the first time on September 14, 2015 [1]. This is the first time that humans have directly observed gravitational wave. In 2017, LIGO and VIRGO announced that three distant gravitational wave detectors detected GW almost simultaneously on August 14, 2017 [2]. However, due to the limited arm length, gravity gradient noise, and seismic noise from the ground, the detection frequency band of ground-based gravitational wave detectors cannot be extended to a lower frequency range. Compared with ground detection of GW, space gravitational wave detection has obvious advantages in terms of wave source type, quantity, signal strength, detectable space distance, etc., and it

The associate editor coordinating the review of this manuscript and approving it for publication was Vittorio Camarchia.

is an irreplaceable observation method for gravitational wave astronomy research. Therefore, the detection of space GW has become a hot spot in the field of space science detection.

Laser Interferometer Space Antenna (LISA) is an all-sky monitor to unveil the Gravitational Universe by detecting GW [3]. LISA's orbit is an Earth-trailing heliocentric orbit between 50 and 65 million km from Earth, with a mean inter-S/C separation distance of 2.5 million km. TianQin is a geocentric space-based GW observatory mission, consisting of three identical drag-free controlled S/C in high Earth orbits at an altitude about 10^5 km, and detect GW in the mHz frequency band [4].

Communication is a key requirement for space gravitational wave detection. On the one hand, the space-based GW detection mission has a long duration, then a large amount of measurement data obtained by GW observatories needs to transmit to the ground for processing in time. On the other hand, the selection of spacecraft orbits will affect its coverage of ground stations, and different communication strategies need to be analyzed and evaluated to ensure the effective transmission of data. According to the nominal mission duration of 4 years in science phase, LISA analyzes the communication requirements for space gravitational wave detection, and enhances the bidirectional laser links between each S/C with data links by modulating data on the pseudo-random code used for ranging [5]. Thus, spacecraft-to-ground data transmission could take place with only one of the three S/C per pass and serve the whole constellation. With this configuration, it has been calculated that communications between a single pointing of one antenna and a single ground station using the X-band can be maintained for 3 days at the rate of $\geq$108.5 kbps, which ensures that the complete 334 MB dataset can be transmitted in less than 7.2 hours. Furthermore, by utilizing multiple ground stations (New Norcia, Cebreros and Malargue), the contact window can be extended to more than 23 hours per day. Different from LISA's heliocentric orbit, TianQin orbit is a geocentric orbit with the geocentric distance of 10^5 km [6]. Consequently, it is necessary for TianQin to explore what communication strategy can be used to transmit data in specific orbital parameters.

In recent years, satellite communication technology has experienced rapid development, thanks to advancements in microelectronics, computer technology, and space science. Addressing the challenges posed by the explosive growth of wireless data traffic in ground cellular networks, particularly in terms of security and energy consumption, the author proposed a collaborative design of the base station's hybrid beamformer and satellite-borne digital beamformer in [7]. This design maximizes confidentiality and energy efficiency. Furthermore, the author achieved multicast communication in satellite aviation integrated networks through technologies such as frequency division multiple access (FDMA), optimizing transmission system rates while satisfying signal-to-noise ratio and power constraints as outlined in [8]. In [9], the author designed a giant satellite-ground integrated network with the potential to achieve seamless global connectivity. In [10], an alternating optimization scheme was proposed to address System Secrecy Energy Efficiency (SEE) by decomposing the original non-convex problem into subproblems. Additionally, in [11], the author utilized Reconfigurable Intelligent Surface (RIS) technology in a satellite-ground hybrid relay network (HSTRN) to enhance communication services, improve HSTRN's Quality of Service (QoS), and reduce the power consumption of the transmission system.

In terms of the satellite communication scheme, it is imperative to analyze the impact of orbit on communication prior to embarking on link design. In space exploration missions, such as Earth observation satellites, earth survey satellites and space stations, Low Earth Orbit (LEO) is commonly employed. Conversely, Middle Earth Orbit (MEO) primarily caters to mobile communications and satellite navigation requirements [12], [13]. Higher geosynchronous orbit (GEO), owing to its synchronization with the angular velocity of the Earth's rotation, is typically utilized for continuous in-orbit measurement and control as well as communication services provision at specific locations [14].

After comprehending the characteristics of the track, executing the link budget work becomes facile. Distinct orbit heights exert diverse influences on communication link design. As orbit height increases, signal propagation extends further and results in amplified propagation loss. Similarly, in LEO and MEO orbits, alterations in the elevation angle of ground stations significantly impact the communication distance between satellites and ground stations [15]. Furthermore, it is imperative to consider factors such as transmission rate and communication frequency band's effects on the link. Latachi, I designed a reliable link to cope with the effects of atmospheric attenuation and Doppler shift effects [16]. Lewark U J analyzed the feasibility of establishing satellite downlink to Earth in E-band [17].

Inevitably encountering attenuation and noise interference within a communication link necessitates optimization for optimal performance. Liu S proposed an adaptive time scale load balancing (ATLB) routing algorithm based on SDN, which has better performance in terms of packet loss rate, end-to-end delay and throughput [18]. Hou C proposed a QoS guaranteed routing strategy to ensure that the route delay and link cost meet the engineering requirements [19].

According to the characteristics of geocentric orbit gravitational wave detection, we analyze the characteristics of satellite and ground station visibility, and design satellite-ground station communication links combining with existing resources, and form several feasible communication schemes for TianQin-Zhuhai. The paper is organized as follows. In Sec. II, we introduce the theoretical model of visibility computation and link budget model. In Sec. III, we describe calculation and simulation analysis under different strategies and modes, In Sec. IV, firstly, the attenuation and gain of X-band and Ka-band in sunny and rainy scenes are meticulously designed and precisely calculated. Moreover,

a comprehensive comparison and analysis is conducted to evaluate the respective merits and demerits of TianQin and LISA in terms of data transmission pertaining to delay, real-time processing, as well as antenna pointing accuracy.

II. THEORETICAL MODEL

A. ORBIT CALCULATION

The TianQin spacecraft orbit is the geocentric ecliptic coordinate system based on J2000 to describe the TianQin spacecraft orbit as Table 1 [20].

TABLE 1. The initial elements TianQin orbits.

	a (km)	e	i(°)	Ω (°)	ω (°)	θ (°)
SC1	100926.	0.000	94.774	209.43	0.9808	84.729
	15846	30	82	301	70	13
SC2	100940.	0.000	94.782	209.43	205.69	359.97
	78902	02	18	045	214	613
SC3	100938.	0.000	94.785	209.43	0.0618	325.61
	05641	41	62	823	31	985

Where, a is the semimajor axis of the orbit, e is the eccentricity, i is the inclination of the orbit, and Ω is the longitude of ascending node. ω is the argument of periapsis, and θ is the true anomaly.

The near-focus coordinate system is a natural coordinate system based on the orbital plane, as shown in Figure 1 with the focus of the orbit as the coordinate origin, the x, y plane as the orbital plane and pointing from the focus to the perigee. The unit vector of the x-axis (arch line) is denoted as $\vec{P}$. The unit vector of the y-axis whose true anomaly angle is 90° with the x-axis is denoted as $\vec{Q}$. The z-axis is perpendicular to the orbital plane and coincides with the direction of the angular momentum h, whose unit vector is denoted as $\vec{W}$.

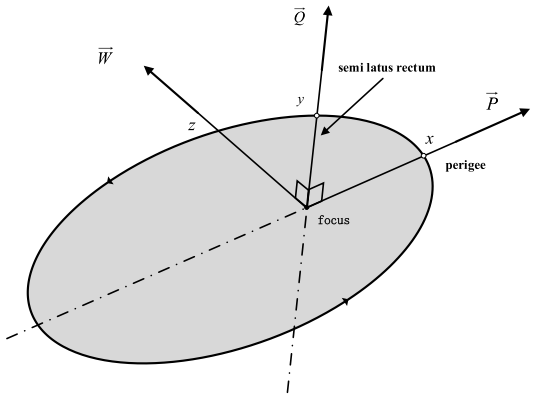

FIGURE 1. The near-focus coordinate system.

In the near-focus coordinate system, the position vector $\vec{r}$ of the spacecraft can be expressed as

$$\vec{r} = r\cos\theta \cdot \vec{P} + r\sin\theta \cdot \vec{Q}\,, \tag{1}$$

in the Eq., the modulus of the $\vec{r}$ can be obtained by the orbital equation

$$r = \frac{h^2}{\mu}\frac{1}{1+e\cos\theta}. \tag{2}$$

Deriving $\vec{r}$, the velocity $\vec{v}$ can be obtained as

$$\vec{v} = \dot{\vec{r}} = -\frac{\mu}{h}\sin\theta \cdot \vec{P} + \frac{\mu}{h}(e+\cos\theta)\cdot\vec{Q}, \tag{3}$$

At the initial time t_0, the position and velocity vectors of the spacecraft can be expressed as

$$\begin{cases} \vec{r}_0 = r_0\cos\theta_0 \cdot \vec{P} + r_0\sin\theta_0 \cdot \vec{Q} \\ \vec{v}_0 = -\dfrac{\mu}{h}\sin\theta_0 \cdot \vec{P} + \dfrac{\mu}{h}(e+\cos\theta_0)\cdot\vec{Q}, \end{cases} \tag{4}$$

$\vec{P}$, $\vec{Q}$ can be calculated

$$\begin{bmatrix} \vec{P} \\ \vec{Q} \end{bmatrix} = \begin{bmatrix} \frac{\mu(e+\cos\theta_0)}{h^2} & -\frac{h\sin\theta_0}{\mu(1+e\cos\theta_0)} \\ \frac{\mu\sin\theta_0}{h^2} & -\frac{h\cos\theta_0}{\mu(1+e\cos\theta_0)} \end{bmatrix} \begin{bmatrix} \vec{r}_0 \\ \vec{v}_0 \end{bmatrix}, \tag{5}$$

Substituting $\vec{P}$ and $\vec{Q}$ into (1) and (2), we can get

$$\begin{bmatrix} \vec{r} \\ \vec{v} \end{bmatrix} = \begin{bmatrix} F(\theta,\theta_0) & G(\theta,\theta_0) \\ F_{\mathrm{t}}(\theta,f_0) & G_{\mathrm{t}}(\theta,\theta_0) \end{bmatrix} \begin{bmatrix} \vec{r}_0 \\ \vec{v}_0 \end{bmatrix}, \tag{6}$$

Among them, function F and function G are called Lagrangian coefficients. According to the Lagrange coefficients, the real-time position prediction of the spacecraft can be performed according to the initial position of the spacecraft from (5) [21].

B. GROUND STATION POSITION CALCULATION

In order to describe the position of the ground station conveniently, it is necessary to introduce a special coordinate system, the geocentric equatorial coordinate system, as shown in Figure 2(a). In the geocentric equatorial coordinate system, the x_{eq}, y_{eq} plane is the equatorial plane, and the x_{eq} axis points to the vernal equinox, and the angle between the y_{eq} axis and the x_c axis in the equatorial plane is 90°, and the z_{eq} axis is perpendicular to the equatorial plane, pointing to the north celestial pole, x_{eq}, y_{eq}, z_{eq} axes form a right-handed system.

The radius of the earth is R_e, at the initial time t_0, the latitude and longitude of the ground station are (φ_P, σ_P), and the altitude of the ground station is h_P, then its coordinates in the geocentric equatorial coordinate system are

$$\vec{P}_{\hat{\mathrm{S}}0} = \begin{pmatrix} (R_{\mathrm{e}}+h_P)\cos\sigma_P\cos\varphi_P, \\ (R_{\mathrm{e}}+h_P)_{\mathrm{e}}\cos\sigma_P\sin\varphi_P, \\ (R_{\mathrm{e}}+h_P)\sin\sigma_P \end{pmatrix}, \tag{7}$$

The earth rotates at a speed of ω_e, after time t, and the coordinates of the ground station in the geocentric equatorial coordinate system are

$$\vec{P}_{\hat{\mathrm{S}}} = \begin{pmatrix} (R_{\mathrm{e}}+h_P)\cos\sigma_P\cos(\sigma_P+\omega_{\mathrm{e}}t), \\ (R_{\mathrm{e}}+h_P)\cos\sigma_P\sin(\sigma_P+\omega_{\mathrm{e}}t), \\ (R_{\mathrm{e}}+h_P)\sin\sigma_P \end{pmatrix}, \tag{8}$$

In order to facilitate position comparison with spacecrafts, it is necessary to unify the coordinates of spacecrafts and

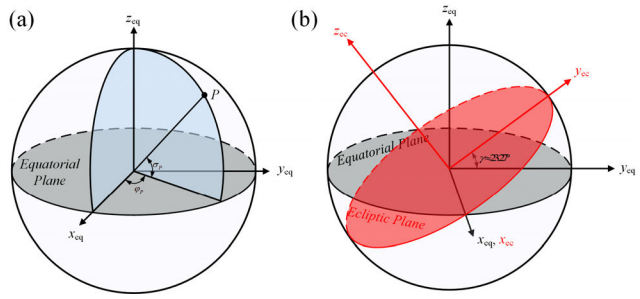

FIGURE 2. Schematic diagram of the geocentric coordinate system.

spacecraft into the same coordinate system. In this paper, the coordinates of the ground station are transformed into the J2000 ecliptic coordinate system that describes the position of the spacecraft. The transformation matrix is

$$Q_{\mathrm{hc}} = \begin{bmatrix} 1 & 0 & 0 \\ 0 & \cos\gamma & \sin\gamma \\ 0 & -\sin\gamma & \cos\gamma \end{bmatrix}, \tag{9}$$

Among them, γ is the angle between the geocentric equatorial coordinate system and the J2000 ecliptic coordinate system, as shown in Figure 2 (b).

From this, the coordinates of the ground station in the J2000 ecliptic coordinate system can be obtained as

$$\vec{P}_{\mathrm{S}} = \gamma \cdot P_{\mathrm{S}}. \tag{10}$$

C. VISIBILITY COMPUTATION

For space-to-ground communication, it is convenient to realize that the spacecraft and the ground station can see each other. In Sec.II-A and Sec. II-B, the real-time positions $\vec{R}$ and $\vec{P}_S$ of the spacecraft and the ground station in the J2000 ecliptic coordinate system are respectively obtained through the calculation. The real-time visibility of the spacecraft and the ground station is judged and analyzed, and the judgment process is as follows.

a. Calculate the relative position of the observatory relative to the spacecraft

$$\vec{W} = \vec{R} - \vec{P}_{\mathrm{S}}. \tag{11}$$

b. Calculate spacecraft elevation angle relative to ground station

$$\sigma = \arccos \frac{\vec{P}_{\mathrm{S}} \cdot \vec{W}}{\left|\vec{P}_{\mathrm{S}} \cdot \vec{W}\right|} - 90^{\circ}. \tag{12}$$

c. Visibility determination

$$\begin{cases} \sigma > \varepsilon \text{ visible} \\ \sigma < \varepsilon \text{ invisible}, \end{cases} \tag{13}$$

among them, $\varepsilon > 0$ is the elevation angle threshold related to the terrain, in this paper, $\varepsilon = 5^{\circ}$.

D. LINK BUDGET MODEL

In the link budget, the gain and attenuation levels of signal and noise are mainly calculated. As shown in (14) [22], we are mainly concerned with the power level of the signal at the receiving end

$$P_r = EIRP + G_r - L, \tag{14}$$

where $EIRP$ is equivalent omnidirectional radiated power, G_r is the gain of the ground station receiving antenna, and L is the various losses involved in the link.

In detail, $EIRP$ is the sum of transmitter transmitting power P_t and transmitting antenna gain G_t, as shown in (15).

$$EIRP = P_t + G_t(\mathrm{dB}). \tag{15}$$

In the link budget, if it is a parabolic antenna, then its antenna gain is

$$G \approx 10\lg(109.66 f^2 d^2 \eta_A)(\mathrm{dB}), \tag{16}$$

where, f, d indicates the carrier frequency, antenna aperture respectively. And η_A indicates the antenna efficiency, which ranges from 55% to 65%.

In this paper, the X-band communication is mainly considered, and the effect of rain failure is not considered for the time being. For other attenuation factors, path attenuation has a greater impact on the link and is related to the communication frequency band and path length.

$$L_{FS} = 20\lg(f) + 20\lg(r) + 92.44(\mathrm{dB}). \tag{17}$$

For the attenuation term, the factors that have a great influence on the link are path attenuation and rainfall attenuation. Among them, rainfall attenuation increases significantly with the increase of communication frequency band. For example, the magnitude of rainfall attenuation in the Ka band (25-40 GHz) is greatly increased compared to the X band (7)-10 GHz).

III. TRANSMISSION TIME CALCULATION BASED ON VISIBILITY ANALYSIS

This section initially introduces three time evaluation indicators, followed by a comprehensive analysis of these indicators in conjunction with the TianQin orbit.

A. DEFINITION OF TIME EVALUATION INDEXES

In order to analyze the communication transmission capability of the communication mode for TianQin, we define three types of evaluation indexes.

1) AVERAGE COMMUNICATION TIME (ACT)

We define the average communication time t_{ACT} as the possible communication time per day between the S/C and the ground station during the scientific mission phase.

2) COMMUNICATION DURATION (CD)

We define the duration of communication t_{CD} as the duration from the beginning to the end of each communication

between the S/C and the ground station. We also use t_{CDmax} and t_{CDmin} to represent the maximum duration and minimum duration during the science mission respectively.

3) DISCONNECTION TIME (DT)

We define the communication disconnection time t_{DT} as the interval between two adjacent communication duration during the scientific mission phase. t_{DTmax} and t_{DTmin} represent the maximum disconnection time and minimum disconnection time respectively.

B. CALCULATION AND ANALYSIS OF TIME EVALUATION INDEXES

1) ACT ANALYSIS

Figure 3 shows that the average communication time between the spacecraft and the ground station is between 11.29 h and 11.42h. In comparison, Jiamusi station has the largest average communication time (11.41 h), followed by Argentina (11.37 h), Kashgar (11.36 h), and finally Zhuhai (11.29 h). For the three spacecraft, the average communication time with the ground station is the same as 11.38h.

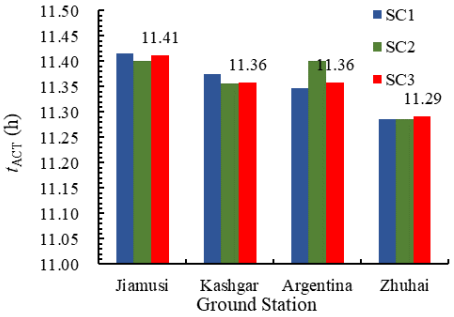

FIGURE 3. ACT of ground stations.

2) CD ANALYSIS

Figure 4-7 shows the CD duration distribution of SC1 in relation to Jiamusi Station, Kashgar Station, Argentina Station and Zhuhai Station respectively. The horizontal axis represents the interval in which the communication duration is located, and the unit is hour. The vertical axis represents the number of occurrences of the corresponding communication duration during the scientific mission phase.

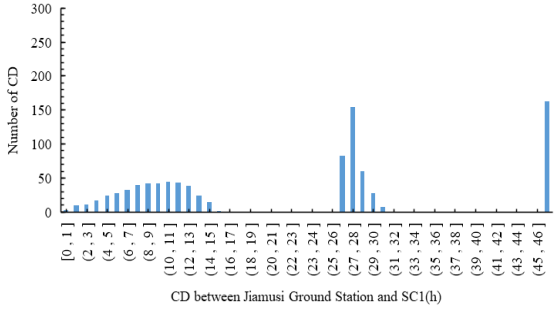

FIGURE 4. CD between Jiamusi ground and SC1.

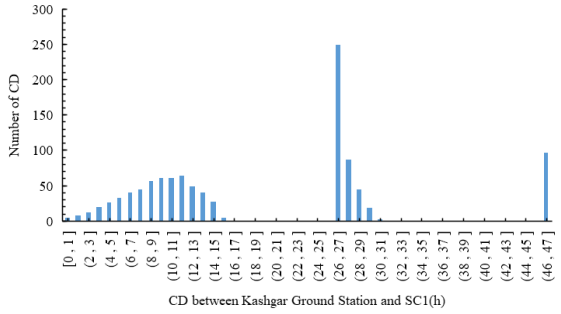

FIGURE 5. CD between Kashgar ground and SC1.

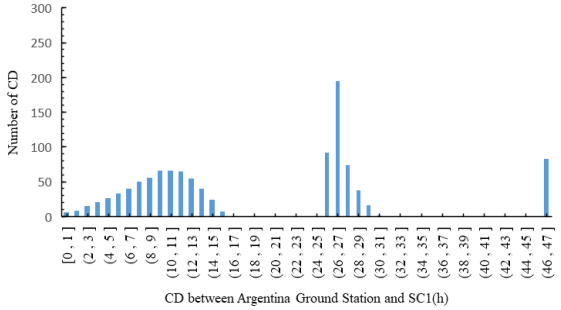

FIGURE 6. CD between Argentina ground and SC1.

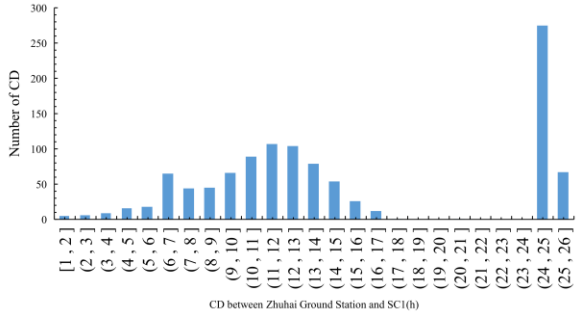

FIGURE 7. CD between Zhuhai ground and SC1.

The data show that under the orbit constraints of TianQin, the communication durations present a regular distribution, and these durations concentrate in three intervals, which is (0, 16), (25, 31) and (45, 47) respectively.

Furthermore, we also found that there is a certain number of short communication durations. Considering the long disconnections before and after these durations, it is difficult to transmit scientific data within the durations. Therefore, we need to reduce the occurrence of short communication durations through ground station selection.

Figure 8(a) illustrates the distribution of the shortest communication duration among the four ground stations, ranging from 0.17 to 1.02 hours. Notably, the ground station in Argentina exhibits the smallest t_{CDmin} distribution, followed by Zhuhai. Figure 8(b) shows that Zhuhai has a significantly

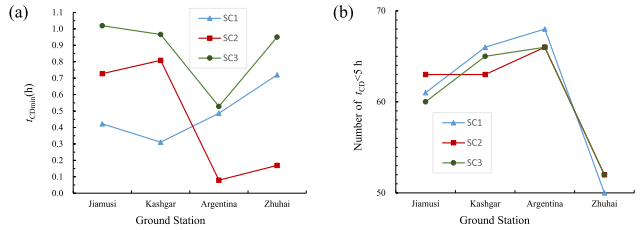

FIGURE 8. Short CD of spacecraft-ground stations.

lower frequency of occurrence for short communication durations (t_{CD} <5 hours) compared to the other three ground stations. Considering that shorter communication times are not conducive to stable data transmission, it can be concluded that Zhuhai ground station is an optimal choice in this regard, with Kashgar ground station being a close second option.

3) DISCONNECTION TIME

The disconnection time can be used to directly analyze the availability of the link between the S/Cs and the ground stations. We obtained the disconnection times during the scientific mission phase, as shown in Figure 9-14. It indicates that the disconnection times distribute in three intervals, which are (0, 17), (27, 32) and (47, 48).

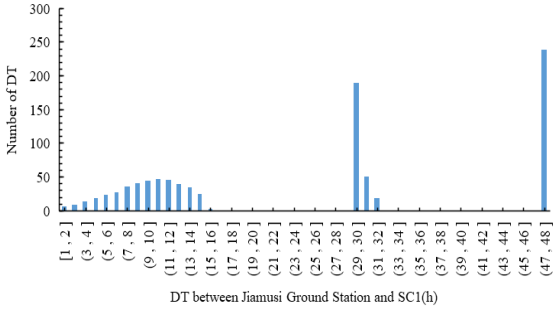

FIGURE 9. DT between Jiamusi ground and SC1.

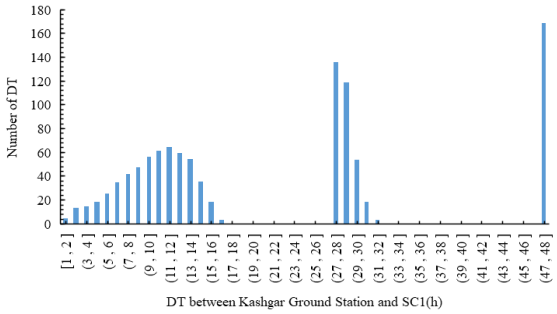

FIGURE 10. DT between Kashgar ground and SC1.

Considering the direct impact of large disconnections on data transmission, we analyze the relationship between the selection of different ground stations and the maximum disconnection time. The disconnection times, which are more than 24 hours, can be divided into two categories, 24h∼35h and 35h∼50h. The statistics data of the two categories are shown in Figure 15. During 24h to 35h, the number of large disconnections of Jiamusi ground station is small, followed by Kashgar ground station, Argentina ground station and Zhuhai ground station. However, during 35h to 50h, Zhuhai ground station appears less frequently, followed by Argentina ground station, Kashgar ground station and Jiamusi ground station. Due to the correlation between large disconnection time and large connection time, it is not advantageous for long-term data transmission to have excessively long or short disconnection times. The data evidence indicates that Zhuhai station exhibits a more evenly distributed connection time, which is conducive to efficient data transmission in the long run.

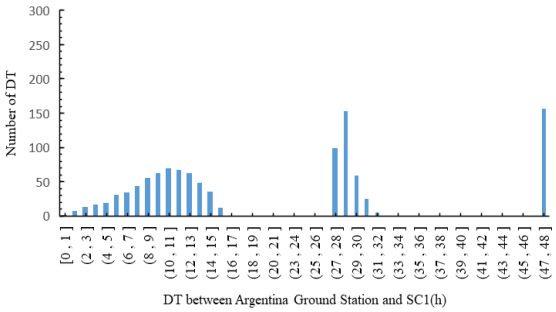

FIGURE 11. DT between Argentina ground and SC1.

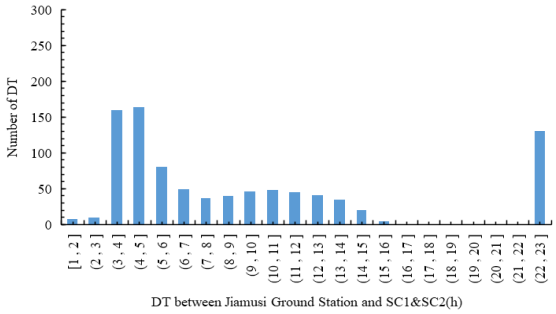

FIGURE 12. DT between Jiamusi ground and SC1&SC2.

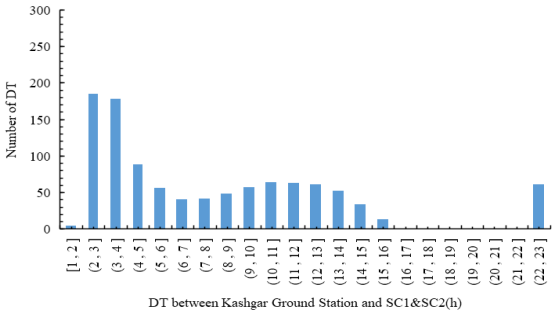

FIGURE 13. DT between Kashgar ground and SC1&SC2.

C. COMPARATIVE ANALYSIS OF GROUND STATIONS

Based on the previous analysis results, it can be concluded that the differences in the average communication time of

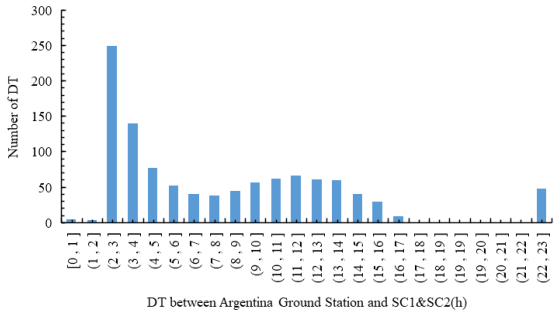

FIGURE 14. DT between Argentina ground and SC1&SC2.

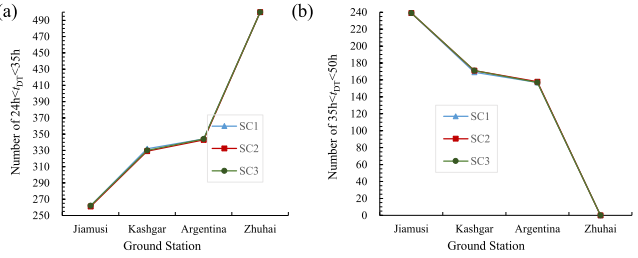

FIGURE 15. Large DT of ground stations.

Kashgar, Jiamusi, Argentina and Zhuhai stations are all within a 7-minute range. However, when considering the distribution of communication time, it is observed that Zhuhai station predominantly exhibits a concentration between 6 to 15 hours. Moreover, occurrences of both short communication times ($\leq$5h) and long disconnection times ($\geq$35h) are infrequent ($\leq$50 times). Consequently, it can be inferred that the communication distribution at Zhuhai station demonstrates greater uniformity compared to other stations. This characteristic is advantageous for designing data transmission schemes and ensuring an organized implementation of data transmission tasks.

IV. COMMUNICATION SCHEME

A. DATA TRANSMISSION REQUIREMENTS OF TIANQIN

When the TianQin satellite is in scientific mode, Data will be generated from Interferometer, Ancillary, Optical Monitoring, GRS Cap.Sens, Drag-Free Attitude Control System(DFACS), etc. According to the sampling rate, sampling depth and sampling channel evaluation, the data generation rate of the TianQin satellite constellation is as shown in Table 2. The data generation rate is expected to be about 41.54 kbit/s for a single satellite and 126kbit/s for the entire constellation. Taking into account satellite overhead such as data coding, the total daily data generated by the entire constellation is approximately 1.62GB based on a 20% margin.

B. COMMUNICATION SCHEME FOR TIANQIN

Since the working distance is 100,000 km away, and the beam antenna can only be aimed at the earth through spacecraft attitude adjustment. As shown in Table 3, we use the Zhuhai

TABLE 2. TianQin data generation rate breakdown.

Parameters	Unit	Quantity
Raw Rate per SC	kbit/s	41.54
Packetization Overhead [20%]	kbit/s	8.31
Packaged Rate per SC	bit/s	49.85
Packaged Rate for Constellation	kbit/s	149.54

TABLE 3. General properties.

Parameters	Unit	Quantity
S/C Dish Diameter	m	0.25
S/C Tx Power	W	50
GS Dish Diameter	m	5
GS G/T	dB/K	35
Data Rate	bps	1,000,000
Other Loss	dB	3

ground station with 5m antenna, which equips with spacecraft receivers of X-band and Ka-band. The spacecraft has an 0.25 m antenna, with transmission power of 50W and transmission rate of 1Mbps.

The preliminary link budget results are shown in Table 4. The main variable is the communication frequency band, which mainly analyzes the different performances of the X-band and Ka-band in the communication link. Among them, compared with the Ka-band, the X-band has the characteristics of longer transmission distance, stronger resistance to atmospheric attenuation and rain attenuation. Compared with the X-band, the Ka-band has a higher bandwidth and can provide a higher transmission rate. In addition, because the Ka-band has a higher frequency, it can bring higher gain under the same antenna aperture. It has greater advantages in

TABLE 4. Communications link budget for TianQin.

Link Parameters	Unit	X-band	Ka-band (sunny)	Ka-band (rainy)
Orbital altitude	km	100000	100000	100000
EIRP	dBW	39.83	50.19	50.20
f	GHz	7.15	33.25	33.25
Free space loss	dB	209.53	222.88	222.88
K	dBW/Hz.K	-228.60	-228.60	-228.60
Atmospheric loss	dB	3.31	0.24	72.95
P_r	dBW	-127.14	-110.71	-183.42
C/N	dBHz	13.55	30.67	-42.04
C/N_0-real	dBHz	75.20	90.67	20.41
E_b/N_0-real	dBHz	15.68	29.33	-43.94
Demodulation loss	dB	2.00	2.00	2.00
C/N_0-need	dBHz	71.60	71.60	71.60
C/N_0 margin	dBHz	4.10	19.08	-53.63

scenarios where server resources are limited. However, while the high frequency brings high gain, if the link transmission encounters rain, it will also bring greater rain attenuation. Additionally, we also calculate the link performance of the Ka-band in sunny and rainy days. It can be seen that if there is no rain attenuation, the Ka-band has significant gains in all aspects of the link.

Judging from the link budget results, there are two options for frequency band selection. Solution 1, directly use the X-band for stable communication at a lower rate. Solution 2, in sunny days, use the Ka-band for high-speed, low-power communication, and in rainy days, use the X-band backup communication link, that is, use the X/Ka frequency band in combination to achieve the maximum communication rate and the lowest communication power consumption. The

Table 4 also reveals that, for the same antenna aperture, Ka-band yields a higher *EIRP* compared to X-band, resulting in an additional antenna gain of 10.36 dB. In sunny conditions, the C/N_0 margin in the Ka band is about 19.08 dBHz, compared to 4.10 dBHz in the X band. It is indicated that at a data rate of 1Mbps, Ka-band could achieve a lower bit error rate. However, during rainfall events, precipitation significantly reduces the C/N_0 margin to -53.63 dBHz in Ka-band which far falls below the demodulation threshold. Considering Zhuhai's meteorological conditions characterized by frequent rainfall and its pronounced impact on Ka-band performance, real-time transmission of gravitational wave data is affected accordingly. Therefore, according to the above link budget analysis, it is recommended to use X-band for TianQin data transmission.

C. COMPARISON WITH LISA COMMUNICATION SCHEME

While both LISA and TianQin share the primary mission objective of detecting GW, their distinct focus areas lead to differences in their orbits and communication strategies, which is show in Table 5. To begin with, LISA orbits in a heliocentric trajectory at a distance of approximately 47∼57 million kilometers, with an arm length of roughly 5 million kilometers, resulting in a communication delay of about 1.67×10^{-1} seconds. On the other hand, TianQin follows a heliocentric orbit at a distance of 10^5 kilometers, resulting in a communication delay of about 3.33×10^{-4} seconds.

TABLE 5. Comparison of communication strategies between TianQin and LISA.

Parameters	TianQin	LISA
Orbital Type	Geocentric orbit	Heliocentric orbit
S/C Tx Frequency	8.45 GHz	8.40 GHz
Data Rate	1 Mps	139 kbps
Transmission Delay	3.33×10^{-4} s	1.67×10^{-1} s
communication duration	24 h	9.2 h
S/C Dish Diameter	0.25 m	0.5 m
Beam Width	10 °	5 °
G/S Dish Diameter	5 m	35 m
C/N_0	75.20 dBHz	55.44 dBHz
Gain Margin	4.10 dB	3 dB

Moreover, concerning visibility analysis outcomes, with both utilizing inter-spacecraft links, LISA experiences an average daily visibility window with the Earth of approximately 9.2 hours per day. In contrast, TianQin can achieve real-time online transmission under inter-spacecraft link conditions. Even in the absence of an inter-spacecraft link, TianQin can reach a communication duration of 11.2 hours per day. Highlight the high practical significance of high-frequency data transmission for multi-messenger observations activities [23].

Finally, due to the characteristics of LISA's orbit, adjustments to antenna pointing are necessary before each communication session. In the context of GW detection, the straight-line antenna alignment of the spacecraft may result in changes to the spacecraft's center of mass, leading to minor deviations in the spacecraft's orbit that could potentially impact the stability of the ranging link. TianQin, situated in a geocentric orbit, can design its antennas to remain consistently pointed towards Earth, mitigating the challenges associated with antenna pointing variations.

V. CONCLUSION

Aiming at the data transmission requirements of gravitational wave detection, this paper establishes a data transmission model of geocentric orbit. Based on the visibility analysis and link budget, several communication comparison schemes of X band and Ka band are given to provide guarantee for the smooth implementation of Tianqin project. Among them, the visibility simulation results show that the average visibility of the four ground stations is 11.29∼11.34 hours/day. Among these stations, Zhuhai has a more uniform distribution of communication time, so it becomes the first choice. In addition, in the link design, combined with the data transmission requirements, we set the transmission rate to 1 Mbps. Furthermore, the link performance under X-band, Ka-band(sunny) and Ka-band(rainy) scenarios are calculated respectively. The results show that although Ka-band can bring greater gain and can meet higher transmission rate, when rain occurs, its C/N_0 margin will drop to -53.63 dBHz, far from meeting the 10^{-5} bit error rate demodulation threshold. Therefore, X-band has better anti-interference performance under the condition of satisfying the basic transmission rate. Finally, the differences between TianQin and LISA in data transmission link are compared and analyzed. The results show that TianQin can achieve lower delay and higher real-time performance in data transmission, which is more conducive to multi-messenger observations activities of major astronomical events. In addition, compared with LISA, TianQin spacecraft does not have the problem of centroid migration caused by the change of spacecraft pointing.

To sum up, due to the different orbital characteristics of TianQin satellite and Tianqin satellite, Tianqin satellite has great advantages in distance attenuation and real-time per-

formance of link signals. Accordingly, we can use smaller resource allocation in TianQin satellite to complete higher speed and higher real-time data transmission.

ACKNOWLEDGMENT

The authors would like to thank Xuefeng Zhang and Bobing Ye for their helpful comments and discussions. They also acknowledge the hospitality of the TianQin Research Center for Gravitational Physics, Sun Yat-sen University.

REFERENCES

[1] F. Marion, "GW150914: Observation of gravitational waves from a binary black hole merger," *Nuovo Cimento C*, vol. 39, no. 4, pp. 310–318, 2016, doi: 10.1393/ncc/i2016-16310-2.

[2] B. P. Abbott, R. Abbott, T. D. Abbott, F. Acernese, K. Ackley, C. Adams, T. Adams, P. Addesso, R. X. Adhikari, V. B. Adya, and C. Affeldt, "GW170817: Observation of gravitational waves from a binary neutron star inspiral," *Phys. Rev. Lett.*, vol. 119, no. 16, 2017, Art. no. 161101.

[3] P. Amaro-Seoane, H. Audley, S. Babak, J. Baker, E. Barausse, P. Bender, E. Berti, P. Binetruy, M. Born, D. Bortoluzzi, and J. Camp, "Laser interferometer space antenna," 2017, *arXiv:1702.00786*.

[4] J. Luo, "A brief introduction to the TianQin project," *Acta Scientiarum Naturalium Universitatis Sunyatseni*, vol. 60, nos. 1–2, pp. 1–19, 2021.

[5] J. J. Esteban, A. F. García, S. Barke, A. M. Peinado, F. G. Cervantes, I. Bykov, G. Heinzel, and K. Danzmann, "Experimental demonstration of weak-light laser ranging and data communication for LISA," *Opt. Exp.*, vol. 19, no. 17, pp. 15937–15946, 2011, doi: 10.1364/oe.19.015937.

[6] B.-B. Ye, X. Zhang, M.-Y. Zhou, Y. Wang, H.-M. Yuan, D. Gu, Y. Ding, J. Zhang, J. Mei, and J. Luo, "Optimizing orbits for TianQin," *Int. J. Modern Phys. D*, vol. 28, no. 9, Jul. 2019, Art. no. 1950121, doi: 10.1142/s0218271819501219.

[7] Z. Lin, M. Lin, B. Champagne, W.-P. Zhu, and N. Al-Dhahir, "Secrecy-energy efficient hybrid beamforming for satellite-terrestrial integrated networks," *IEEE Trans. Commun.*, vol. 69, no. 9, pp. 6345–6360, Sep. 2021, doi: 10.1109/TCOMM.2021.3088898.

[8] Z. Lin, M. Lin, T. de Cola, J.-B. Wang, W.-P. Zhu, and J. Cheng, "Supporting IoT with rate-splitting multiple access in satellite and aerial-integrated networks," *IEEE Internet Things J.*, vol. 8, no. 14, pp. 11123–11134, Jul. 2021, doi: 10.1109/JIOT.2021.3051603.

[9] P. Wang, B. Di, and L. Song, "Mega-constellation design for integrated satellite-terrestrial networks for global seamless connectivity," *IEEE Wireless Commun. Lett.*, vol. 11, no. 8, pp. 1669–1673, Aug. 2022, doi: 10.1109/LWC.2022.3171574.

[10] Z. Lin, K. An, H. Niu, Y. Hu, S. Chatzinotas, G. Zheng, and J. Wang, "SLNR-based secure energy efficient beamforming in multibeam satellite systems," *IEEE Trans. Aerosp. Electron. Syst.*, vol. 59, no. 2, pp. 2085–2088, Apr. 2023, doi: 10.1109/TAES.2022.3190238.

[11] Z. Lin, H. Niu, K. An, Y. Wang, G. Zheng, S. Chatzinotas, and Y. Hu, "Refracting RIS-aided hybrid satellite-terrestrial relay networks: Joint beamforming design and optimization," *IEEE Trans. Aerosp. Electron. Syst.*, vol. 58, no. 4, pp. 3717–3724, Aug. 2022, doi: 10.1109/TAES.2022.3155711.

[12] O. Kodheli, E. Lagunas, N. Maturo, S. K. Sharma, B. Shankar, J. F. M. Montoya, J. C. M. Duncan, D. Spano, S. Chatzinotas, S. Kisseleff, J. Querol, L. Lei, T. X. Vu, and G. Goussetis, "Satellite communications in the new space era: A survey and future challenges," *IEEE Commun. Surveys Tuts.*, vol. 23, no. 1, pp. 70–109, 1st Quart., 2021, doi: 10.1109/COMST.2020.3028247.

[13] Y. Yang, L. Liu, J. Li, Y. Yang, T. Zhang, Y. Mao, B. Sun, and X. Ren, "Featured services and performance of BDS-3," *Sci. Bull.*, vol. 66, no. 20, pp. 2135–2143, Oct. 2021, doi: 10.1016/j.scib.2021.06.013.

[14] A. Monti Guarnieri, A. Broquetas, A. Recchia, F. Rocca, and J. Ruiz-Rodon, "Advanced radar geosynchronous observation system: Argos," *IEEE Geosci. Remote Sens. Lett.*, vol. 12, no. 7, pp. 1406–1410, Jul. 2015, doi: 10.1109/LGRS.2015.2404214.

[15] J. M. Gongora-Torres, C. Vargas-Rosales, A. Aragón-Zavala, and R. Villalpando-Hernandez, "Link budget analysis for LEO satellites based on the statistics of the elevation angle," *IEEE Access*, vol. 10, pp. 14518–14528, 2022, doi: 10.1109/ACCESS.2022.3147829.

[16] I. Latachi, M. Karim, A. Hanafi, T. Rachidi, A. Khalayoun, N. Assem, S. Dahbi, and S. Zouggar, "Link budget analysis for a LEO cubesat communication subsystem," in *Proc. Int. Conf. Adv. Technol. Signal Image Process. (ATSIP)*, May 2017, pp. 1–6.

[17] U. J. Lewark, J. Antes, J. Walheim, J. Timmermann, T. Zwick, and I. Kallfass, "Link budget analysis for future E-band gigabit satellite communication links (71–76 and 81–84 Ghz)," *CEAS Space J.*, vol. 4, nos. 1–4, pp. 41–46, Jun. 2013, doi: 10.1007/s12567-013-0030-0.

[18] S. Liu, J. Liu, and B. Xia, "Adaptive timescale load balancing routing algorithm for LEO satellite network," in *Proc. IEEE/CIC Int. Conf. Commun. China (ICCC)*, Aug. 2023, pp. 1–5.

[19] C. Hou and Y. Zhu, "The QoS guaranteed routing strategy in low Earth orbit satellite constellations," in *Proc. IEEE/CIC Int. Conf. Commun. China (ICCC Workshops)*, Aug. 2023, pp. 1–6.

[20] B. Ye, X. Zhang, Y. Ding, and Y. Meng, "Eclipse avoidance in TianQin orbit selection," *Phys. Rev. D*, vol. 103, no. 4, Feb. 2021, Art. no. 042007, doi: 10.1103/physrevd.103.042007.

[21] H. D. Curtis, "Orbital position as a function of time," in *Orbital Mechanics for Engineering Student*. U.K.: Butterworth-Heineman, 2013, pp. 107–145.

[22] L. J. Ippolito Jr., *Satellite Communications Systems Engineering: Atmospheric Effects, Satellite Link Design and System Performance*. Hoboken, NJ, USA: Wiley, 2017.

[23] H. Tong, M.-X. Liu, Y.-M. Hu, M. Leong Chan, M. Hendry, Z. Liu, and H. Sun, "Following up the afterglow: Strategy for X-ray observation triggered by gravitational wave events," 2020, *arXiv:2005.11076*.

ZHAOXIANG YI received the M.Sc. and Ph.D. degrees in computer application from Xi'an High-Tech Research Institute. In 2020, he joined the TianQin Research Center for Gravitational Physics, Sun Yat-sen University, to conduct research on inter-satellite laser communication and satellite-ground communication in space gravitational wave detection. His research interests include communication systems, satellite communications, computer simulation, and intelligent information processing. He is a Senior Member of the China Computer Society. He is the Director of the China Association of Computer Automated Measurement and Control Technology.

LIN SUN (Graduate Student Member, IEEE) received the B.Sc. degree from Sichuan Agricultural University. He is currently pursuing the M.Sc. degree with the TianQin Research Center for Gravitational Physics, Sun Yat-sen University. His research interests include satellite communication, space communications, signal processing, and gravitational wave detection.

MENG JIANG (Graduate Student Member, IEEE) received the B.Eng. degree from Sichuan Agricultural University. She is currently pursuing the M.Sc. degree with the TianQin Research Center for Gravitational Physics, Sun Yat-sen University. Her research interests include space communication and space ranging.